LAWRENCE
LIVERMORE
NATIONAL
LABORATORY

Wave-Based Inversion & Imaging for the Optical Quadrature Microscope

S. K. Lehman

November 14, 2005

Disclaimer

Wave-Based Inversion & Imaging for the Optical Quadrature Microscope

Sean K. Lehman

November 14, 2005

Abstract

The Center for Subsurface Sensing & Imaging System's (CenSSIS) Optical Quadrature Microscope (OQM) is a narrow band visible light microscope capable of measuring both amplitude and phase of a scattered field. We develop a diffraction tomography, that is, wave-based, scattered field inversion and imaging algorithm, for reconstructing the refractive index of the scattering object.

UCRL-TR-217047

Contents

1 Introduction

The Center for Subsurface Sensing & Imaging System's (CenSSIS) Optical Quadrature Microscope (OQM) is a narrow band visible light microscope capable of measuring both amplitude and phase of a scattered field. We develop a diffraction tomography, that is, wave-based, scattered field inversion and imaging algorithm, for reconstructing the refractive index of the scattering object.

   The purposes of this report is to develop a wave-based inversion and imaging algorithm, not to describe the OQM. We refer the reader to the references [1, 2, 3, 4, 5] for a thorough development of the OQM. Our fundamental assumption, here, is that the OQM can measure a fully complex field (simultaneously measure the magnitude and phase of a scattered field) at a single measurement plane. We also assume the incident field is planar and that both it and measurement plane are rotated about the scattering object (object under evaluation) at multiple angular locations uniformly distributed over $360°$ as indicated in Figure 1.

   We develop our forward scattering model in the next section including derivations under the Born (amplitude) and Rytov (phase) approximations. The inversion algorithm is described in Section 3.

2 Total Field Propagation

We begin by considering the wave equation

$$\left[\nabla^2 - \frac{n^2(\mathbf{r})}{c_0^2}\partial_t^2\right]\psi^{tot}(\mathbf{r}, \mathbf{R}_n^t, t) = -p(\mathbf{r}, \mathbf{R}_n^t, t), \tag{1}$$

in which we have assumed a variable medium through the *refractive index*

$$n(\mathbf{r}) \equiv \frac{c_0}{c(\mathbf{r})}. \tag{2}$$

$n(\mathbf{r})$ to represents the presence of a scattering object, that is, the object under evaluation. $\psi^{tot}(\mathbf{r}, \mathbf{R}_n^t, t)$ is the *total field* (the sum of the scattered and incident fields), $p(\mathbf{r}, \mathbf{R}_n^t, t)$ is the incident pulse applied to the n-th transmitter located at $\mathbf{R}_n^t$, and c_0 is the background wave speed. We Fourier transform Eqn. 1 using the temporal transform of Appendix A:

$$\left[\nabla^2 + k_0^2 n^2(\mathbf{r})\right]\psi^{tot}(\mathbf{r}, \mathbf{R}_n^t, \omega) = -p(\mathbf{r}, \mathbf{R}_n^t, \omega), \tag{3}$$

where the *background wavenumber* is defined as

$$k_0 \equiv \frac{\omega}{c_0}.$$

   When solving the forward problem, it is frequently convenient to cast Eqn. 3 into an integral equation. We do so by adding $k_0\psi^{tot}(\mathbf{r}, \mathbf{R}_n^t, \omega)$ to both sides of Eqn. 3, and moving the inhomogeneous term to the right hand side:

$$\left[\nabla^2 + k_0^2\right]\psi^{tot}(\mathbf{r}, \mathbf{R}_n^t, \omega) = -p(\mathbf{r}) - \left[k_0^2 n^2(\mathbf{r}) - k_0^2\right]\psi^{tot}(\mathbf{r}, \mathbf{R}_n^t, \omega). \tag{4}$$

Define the *object function* as

$$o(\mathbf{r}) \equiv n^2(\mathbf{r}) - 1, \tag{5}$$

and express Eqn. 4 as

$$\left[\nabla^2 + k_0^2\right] \psi^{tot}(\mathbf{r}, \mathbf{R}_n^t, \omega) = -p(\mathbf{r}, \mathbf{R}_n^t, \omega) - k_0^2 o(\mathbf{r}) \psi^{tot}(\mathbf{r}, \mathbf{R}_n^t, \omega). \tag{6}$$

The first term on the right-hand side of Eqn. 6, $p(\mathbf{r}, \mathbf{R}_n^t, \omega)$, is the *primary source*. The second, source-like, term on the right-hand side, $k_0^2 o(\mathbf{r}) \psi^{tot}(\mathbf{r}, \mathbf{R}_n^t, \omega)$, is known as the *secondary source*. We may use Green's theorem to cast the differential equation of Eqn. 6 into an integral equation [6],

$$\psi^{tot}(\mathbf{r}, \mathbf{R}_n^t, \omega) = \underbrace{\int d\mathbf{r}' \, G_0(\mathbf{r}, \mathbf{r}', \omega) \, p(\mathbf{r}', \mathbf{R}_n^t, \omega)}_{\psi^{inc}(\mathbf{r}, \mathbf{R}_n^t, \omega)} +$$

$$\underbrace{k_0^2 \int d\mathbf{r}' \, G_0(\mathbf{r}, \mathbf{r}', \omega) \, o(\mathbf{r}') \, \psi^{tot}(\mathbf{r}', \mathbf{R}_n^t, \omega)}_{\psi^{scat}(\mathbf{r}, \mathbf{R}_n^t, \omega)}, \tag{7}$$

where the background Green function satisfies

$$\left[\nabla^2 + k_0^2\right] G_0(\mathbf{r}, \mathbf{r}', \omega) = -\delta(\mathbf{r} - \mathbf{r}'). \tag{8}$$

We define the *primary*, *incident*, or *background* field as

$$\psi^{inc}(\mathbf{r}, \mathbf{R}_n^t, \omega) \equiv \int d\mathbf{r}' \, G_0(\mathbf{r}, \mathbf{r}', \omega) \, p(\mathbf{r}', \mathbf{R}_n^t, \omega), \tag{9}$$

so that Eqn. 7 reads

$$\psi^{tot}(\mathbf{r}, \mathbf{R}_n^t, \omega) = \psi^{inc}(\mathbf{r}, \mathbf{R}_n^t, \omega) + k_0^2 \int d\mathbf{r}' \, G_0(\mathbf{r}, \mathbf{r}', \omega) \, o(\mathbf{r}') \, \psi^{tot}(\mathbf{r}', \mathbf{R}_n^t, \omega). \tag{10}$$

The *scattered field* is then defined as the difference between the total and incident fields,

$$\psi^{scat}(\mathbf{r}, \mathbf{R}_n^t, \omega) \equiv \psi^{tot}(\mathbf{r}, \mathbf{R}_n^t, \omega) - \psi^{inc}(\mathbf{r}, \mathbf{R}_n^t, \omega)$$
$$= k_0^2 \int d\mathbf{r}' \, G_0(\mathbf{r}, \mathbf{r}', \omega) \, o(\mathbf{r}') \, \psi^{tot}(\mathbf{r}', \mathbf{R}_n^t, \omega). \tag{11}$$

We observe that with the primary field satisfying

$$\left[\nabla^2 + k_0^2\right] \psi^{inc}(\mathbf{r}, \mathbf{R}_n^t, \omega) = -p(\mathbf{r}, \mathbf{R}_n^t, \omega), \tag{12}$$

the scattered field obeys

$$\left[\nabla^2 + k_0^2\right] \psi^{scat}(\mathbf{r}, \mathbf{R}_n^t, \omega) = -k_0^2 o(\mathbf{r}) \psi^{tot}(\mathbf{r}, \mathbf{R}_n^t, \omega), \tag{13}$$

or alternatively,

$$\left[\nabla^2 + k_0^2 n^2(\mathbf{r})\right]\psi^{scat}(\mathbf{r}, \mathbf{R}_n^t, \omega) = -k_0^2 o(\mathbf{r})\psi^{inc}(\mathbf{r}, \mathbf{R}_n^t, \omega). \tag{14}$$

The integral equation of Eqn. 11 is non-linear in that the scattered field appears in both sides of the equation. The differential equation of Eqn. 14 offers the problem of having spatially dependent scattering operator. Exact analytic solutions for the scattered field exist only for a limited set of scattering objects. Numerical solutions are readily available but not appropriate for an arbitrary object tomographic inversion algorithm. Thus, we wish to simplify our forward model. In the following section we simplify the model under the Born approximation. In Section 2.2 use the Rytov approximation. We note that the Born and Rytov approximations are the two most practical simplifications when little is known of the scattering object. When more is known of the object, this prior information can be included in the model via a modified Green function or through a model-based processing approach and an (fast) forward propagator.

2.1 Born Approximation

One potential method of simplifying Eqn. 14 for solving is to use a perturbation approach. We express the refractive index and scattered field as [7]

$$n^2(\mathbf{r}) = n_0^2(\mathbf{r}) + \underbrace{\epsilon n_1(\mathbf{r}) + \epsilon^2 n_2(\mathbf{r}) + \cdots}_{\equiv\, \delta n(\mathbf{r})}, \tag{15}$$

$$\psi^{scat}(\mathbf{r}, \mathbf{R}_n^t, \omega) = \psi^{scat}_{DWB}(\mathbf{r}, \mathbf{R}_n^t, \omega) + \epsilon\psi_1^{scat}(\mathbf{r}, \mathbf{R}_n^t, \omega) + \epsilon^2\psi_2^{scat}(\mathbf{r}, \mathbf{R}_n^t, \omega) + \cdots,$$

respectively, substitute them into Eqn. 14, and equate like powers of ϵ. Doing so we obtain the follow set of equations:

$$\left[\nabla^2 + k_0^2 n_0^2(\mathbf{r})\right]\psi^{scat}_{DWB}(\mathbf{r}, \mathbf{R}_n^t, \omega) = -k_0^2 o(\mathbf{r})\psi^{inc}(\mathbf{r}, \mathbf{R}_n^t, \omega), \tag{16}$$

$$\left[\nabla^2 + k_0^2 n_0^2(\mathbf{r})\right]\psi_1^{scat}(\mathbf{r}, \mathbf{R}_n^t, \omega) = -k_0^2 n_1(\mathbf{r})\psi^{scat}_{DWB}(\mathbf{r}, \mathbf{R}_n^t, \omega), \tag{17}$$

$$\left[\nabla^2 + k_0^2 n_0^2(\mathbf{r})\right]\psi_2^{scat}(\mathbf{r}, \mathbf{R}_n^t, \omega) = -k_0^2 n_2(\mathbf{r})\psi^{scat}_{DWB}(\mathbf{r}, \mathbf{R}_n^t, \omega)$$
$$-k_0^2 n_1(\mathbf{r})\psi_1^{scat}(\mathbf{r}, \mathbf{R}_n^t, \omega), \tag{18}$$

$$\vdots$$

$$\left[\nabla^2 + k_0^2 n_0^2(\mathbf{r})\right]\psi_l^{scat}(\mathbf{r}, \mathbf{R}_n^t, \omega) = -k_0^2 \sum_{m=0}^{l-1} n_{l-m}(\mathbf{r})\psi_m^{scat}(\mathbf{r}, \mathbf{R}_n^t, \omega). \tag{19}$$

The Green function for the left hand side operators of Eqns. 16 through 18 satisfies

$$\left[\nabla^2 + k_0^2 n_0^2(\mathbf{r})\right]G(\mathbf{r}, \mathbf{r}', \omega) = -\delta(\mathbf{r} - \mathbf{r}'). \tag{20}$$

Note: this is not the background Green function of Eqn. 8. Using this to cast Eqn. 16 into an integral equation, we obtain the *distorted wave Born approximation* to the scattered field,

$$\psi^{scat}_{DWB}(\mathbf{r}, \mathbf{R}_n^t, \omega) = k_0^2 \int d\mathbf{r}'\, G(\mathbf{r}, \mathbf{r}', \omega)\, o(\mathbf{r}')\, \psi^{inc}(\mathbf{r}', \mathbf{R}_n^t, \omega). \tag{21}$$

3

When $n_0(\mathbf{r}) \equiv 1$, this reduces to the standard *Born approximation* [8],

$$\psi_B^{scat}(\mathbf{r}, \mathbf{R}_n^t, \omega) = k_0^2 \int d\mathbf{r}' \, G_0(\mathbf{r}, \mathbf{r}', \omega) \, o(\mathbf{r}') \, \psi^{inc}(\mathbf{r}', \mathbf{R}_n^t, \omega). \tag{22}$$

Comparing this to Eqn. 11, we see the Born approximation effectively replaces the total field with the incident field.

2.2 Rytov Approximation

The Rytov approximation [8] starts with Eqn. 6 and the assumptions that the source term is either identically zero (accurate if we consider a volume which excludes the source support),

$$p(\mathbf{r}, \mathbf{R}_n^t, \omega) \equiv 0, \tag{23}$$

or a plane wave with propagation vector $\hat{\mathbf{s}}$,

$$p(\mathbf{r}, \hat{\mathbf{s}}, \omega) \equiv P(\omega) \, e^{ik_0 \hat{\mathbf{s}} \cdot \mathbf{r}}; \tag{24}$$

and that the total field can be expressed as

$$\psi^{tot}(\mathbf{r}) = \psi^{inc}(\mathbf{r}) \psi^{scat}(\mathbf{r}) = e^{\phi_i(\mathbf{r})} e^{\phi_s(\mathbf{r})}, \tag{25}$$

where $\phi_i(\mathbf{r})$ and $\phi_s(\mathbf{r})$ are the incident and scattered field complex phases, respectively, and the total phase is

$$\phi(\mathbf{r}) = \phi_i(\mathbf{r}) + \phi_s(\mathbf{r}). \tag{26}$$

For this section, we omit the explicit dependence of the fields on the temporal frequency, ω, and references to the incident field ($\mathbf{R}_n^t$ for a point source, or $\hat{\mathbf{s}}$ for a plane wave). We have the following identities

$$\nabla \psi^{tot}(\mathbf{r}) = \psi^{tot}(\mathbf{r}) \nabla \phi(\mathbf{r}), \tag{27}$$

$$\nabla^2 \psi^{tot}(\mathbf{r}) = \psi^{tot}(\mathbf{r}) \left[\nabla^2 \phi(\mathbf{r}) + (\nabla \phi(\mathbf{r}))^2 \right]. \tag{28}$$

Using Eqn. 28, Eqn. 6 reads,

$$\nabla^2 \phi(\mathbf{r}) + (\nabla \phi(\mathbf{r}))^2 + k_0^2 = -k_0^2 o(\mathbf{r}), \tag{29}$$

which reduces to

$$\nabla^2 \phi(\mathbf{r}) + (\nabla \phi(\mathbf{r}))^2 = -k_0^2 n^2(\mathbf{r}), \tag{30}$$

where we have used the definition of the object function from Eqn. 5.

4

As in the Born approximation development, we expand the object function and total phase as follows,

$$n^2(\mathbf{r}) = n_0^2(\mathbf{r}) + \underbrace{\epsilon n_1(\mathbf{r}) + \epsilon^2 n_2(\mathbf{r}) + \cdots}_{\equiv \, \delta n(\mathbf{r})},$$ (31)

$$\phi(\mathbf{r}) = \phi_i(\mathbf{r}) + \epsilon \phi_1^{scat}(\mathbf{r}) + \epsilon^2 \phi_2^{scat}(\mathbf{r}) + \cdots.$$

Substituting the expansions from Eqn. 31 into Eqn. 30 and collecting powers of ϵ, we find

$$\nabla^2 \phi_i + (\nabla \phi_i)^2 = -k_0^2 n_0^2(\mathbf{r}),$$ (32)

$$\nabla^2 \phi_1 + 2 \nabla \phi_i \cdot \nabla \phi_1 = -k_0^2 n_1(\mathbf{r}),$$ (33)

$$\nabla^2 \phi_2 + 2 \nabla \phi_i \cdot \nabla \phi_2 = -k_0^2 n_2(\mathbf{r}) - (\nabla \phi_1)^2,$$ (34)

$$\nabla^2 \phi_3 + 2 \nabla \phi_i \cdot \nabla \phi_3 = -k_0^2 n_3(\mathbf{r}) - 2 \nabla \phi_1 \cdot \nabla \phi_2,$$ (35)

$$\vdots$$

$$\nabla^2 \phi_l + 2 \nabla \phi_i \cdot \nabla \phi_l = -k_0^2 n_l(\mathbf{r}) - \sum_{m=1}^{l-1} \nabla \phi_m \cdot \nabla \phi_{l-m}.$$ (36)

Consider

$$\nabla^2 \left(\psi^{inc}(\mathbf{r}) \phi_s(\mathbf{r}) \right) = \left(\psi^{inc}(\mathbf{r}) \phi_s(\mathbf{r}) \right) \left[(\nabla \phi_i(\mathbf{r}))^2 + \nabla^2 \phi_i(\mathbf{r}) \right]$$
$$+ \psi^{inc}(\mathbf{r}) \left[2 \nabla \phi_i(\mathbf{r}) \cdot \nabla \phi_s(\mathbf{r}) + \nabla^2 \phi_s(\mathbf{r}) \right].$$ (37)

Substituting Eqn. 32 and re-arranging terms, yields

$$\left[\nabla^2 + k_0^2 n_0^2(\mathbf{r}) \right] \left(\psi^{inc}(\mathbf{r}) \phi_s(\mathbf{r}) \right) = \psi^{inc}(\mathbf{r}) \left[2 \nabla \phi_i(\mathbf{r}) \cdot \nabla \phi_s(\mathbf{r}) + \nabla^2 \phi_s(\mathbf{r}) \right].$$ (38)

Retaining only the first two terms in the expansion of Eqn. 31,

$$n^2(\mathbf{r}) \approx n_0^2(\mathbf{r}) + n_1(\mathbf{r}),$$
$$\phi(\mathbf{r}) \approx \phi_i(\mathbf{r}) + \phi_1^{scat}(\mathbf{r}) \equiv \phi_i(\mathbf{r}) + \phi_s(\mathbf{r}),$$ (39)

and using Eqn. 33, we obtain the *distorted wave Rytov approximation*,

$$\left[\nabla^2 + k_0^2 n_0^2(\mathbf{r}) \right] \left(\psi^{inc}(\mathbf{r}) \phi_s(\mathbf{r}) \right) = -k_0^2 n_1(\mathbf{r}) \psi^{inc}(\mathbf{r}).$$ (40)

Using Eqn. 20, we cast this into an integral equation

$$\phi_s(\mathbf{r}) = \frac{k_0^2}{\psi^{inc}(\mathbf{r})} \int d\mathbf{r}' \, G(\mathbf{r}, \mathbf{r}', \omega) \, n_1(\mathbf{r}') \, \psi^{inc}(\mathbf{r}').$$ (41)

From Eqn. 39, we observe that

$$n_1(\mathbf{r}) \approx n^2(\mathbf{r}) - n_0^2(\mathbf{r}).$$ (42)

When $n_0(\mathbf{r}) \equiv 1$, Eqn. 41 reduces to the classical *Rytov approximation*,

$$\phi_s(\mathbf{r}) = \frac{k_0^2}{\psi^{inc}(\mathbf{r})} \int d\mathbf{r}' \, G_0(\mathbf{r}, \mathbf{r}', \omega) \, o(\mathbf{r}') \, \psi^{inc}(\mathbf{r}').$$ (43)

2.3 Summary of Born & Rytov Approximations

The forward scattering equations for the Born and Rytov approximations have identical forms for the quantity they approximate: the scattered amplitude for the former, and the scattered phase for the latter. We repeat them here,

$$\psi_B^{scat}(\mathbf{r}, \mathbf{R}_n^t, \omega) \;=\; k_0^2 \int d\mathbf{r}' \, G_0(\mathbf{r}, \mathbf{r}', \omega) \, o(\mathbf{r}') \, \psi^{inc}(\mathbf{r}', \mathbf{R}_n^t, \omega), \tag{44}$$

$$\phi_s(\mathbf{r}) \;=\; \frac{k_0^2}{\psi^{inc}(\mathbf{r})} \int d\mathbf{r}' \, G_0(\mathbf{r}, \mathbf{r}', \omega) \, o(\mathbf{r}') \, \psi^{inc}(\mathbf{r}'). \tag{45}$$

We may compactly express these two equations as

$$U^{scat}(\mathbf{r}) \;=\; C(\mathbf{r}) \, k_0^2 \int d\mathbf{r}' \, G_0(\mathbf{r}, \mathbf{r}', \omega) \, o(\mathbf{r}') \, \psi^{inc}(\mathbf{r}'), \tag{46}$$

where we have the following definitions

$$U^{scatt}(\mathbf{r}) \;\equiv\;
\begin{cases}
\psi_B^{scat}(\mathbf{r}, \mathbf{R}_n^t, \omega) & \text{for the Born approximation,} \\[2mm]
\phi_s(\mathbf{r}) & \text{for the Rytov approximation,}
\end{cases} \tag{47}$$

$$C(\mathbf{r}) \;\equiv\;
\begin{cases}
1 & \text{for the Born approximation,} \\[2mm]
\dfrac{1}{\psi^{inc}(\mathbf{r})} & \text{for the Rytov approximation.}
\end{cases} \tag{48}$$

2.4 Incident Fields

Usually, the incident field is taken to be either a plane with unit propagation vector $\hat{\mathbf{s}}$ or spherical wave due to a point source located at $\mathbf{R}_n^t$. We express these mathematically as

$$\psi^{inc}(\mathbf{r}) \;=\;
\begin{cases}
P(\omega) \, e^{ik_0 \hat{\mathbf{s}} \cdot \mathbf{r}} & \text{plane wave,} \\[2mm]
P(\omega) \, G_0(\mathbf{r}, \mathbf{R}_n^t, \omega) & \text{spherical wave,}
\end{cases} \tag{49}$$

where $P(\omega)$ is the temporal spectrum of the incident field, and $G(\mathbf{r}, \mathbf{r}', \omega)$ is the Green function response of the medium.

We summarize the forward models of Eqn. 46 as follows:

$$U^{scat}(\mathbf{r}, \hat{\mathbf{s}}) \;=\; C(\mathbf{r}) \, P(\omega) \, k_0^2 \int d\mathbf{r}' \, G_0(\mathbf{r}, \mathbf{r}', \omega) \, o(\mathbf{r}') \, e^{ik_0 \hat{\mathbf{s}} \cdot \mathbf{r}'}, \tag{50}$$

$$U^{scat}(\mathbf{r}, \mathbf{R}^t) \;=\; C(\mathbf{r}) \, P(\omega) \, k_0^2 \int d\mathbf{r}' \, G_0(\mathbf{r}, \mathbf{r}', \omega) \, o(\mathbf{r}') \, G_0(\mathbf{r}', \mathbf{R}^t, \omega). \tag{51}$$

With our forward models in hand, we are now prepared to develop a method for inverting them to determine the scattering object based upon a set of scattered field measurements. We derive the "classical" plane wave diffraction tomography algorithm [9] in the following section.

3 Inversion Using Incident Plane Wave and Planar Measurement

Eqns. 50 and 51 represent two possible forward models depending upon the nature of the probing source (either plane wave or point). The measurement system rotates about the fixed object. We label the *fixed object coordinate system* by $\mathbf{R} \equiv (X, Y, Z)$. The axis of rotation is the Y-axis. The *rotated coordinate system* is defined by $\mathbf{r} \equiv (x, y, z) = (-Z \sin \theta + X \cos \theta, 0, Z \cos \theta + X \sin \theta)$. The relationship between the two coordinate systems is given by

$$
\begin{bmatrix} x \\ y \\ z \end{bmatrix} = \begin{bmatrix} \cos \theta & 0 & -\sin \theta \\ 0 & 1 & 0 \\ \sin \theta & 0 & \cos \theta \end{bmatrix} \begin{bmatrix} X \\ Y \\ Z \end{bmatrix}
\tag{52}
$$

We take the z-axis to be the major alignment axis of the measurement system. We assume a planar measurement surface located at $z = z_p$ whose normal lies along the z-axis:

$$
\mathbf{R}^r = (x, y, z_p) = (\mathbf{r}_\perp, z_p).
$$

A schematic of the measurement system is presented in Figure 1.

For future reference, the complementary rotated spatial Fourier variables are defined by

$$
\begin{aligned}
\mathbf{k} \cdot \mathbf{r} &= k_x x + k_y y + k_z z, \\
&= k_x (X \cos \theta - Z \sin \theta) + k_y y + k_z (X \sin \theta + Z \cos \theta), \\
&= (k_x \cos \theta + k_z \sin \theta) X + k_y Y + (-k_x \sin \theta + k_z \cos \theta) Z, \\
&= \mathbf{K} \cdot \mathbf{R},
\end{aligned}
\tag{53}
$$

so that we have

$$
\begin{bmatrix} K_x \\ K_y \\ K_z \end{bmatrix} = \begin{bmatrix} \cos \theta & 0 & \sin \theta \\ 0 & 1 & 0 \\ -\sin \theta & 0 & \cos \theta \end{bmatrix} \begin{bmatrix} k_x \\ k_y \\ k_z \end{bmatrix}.
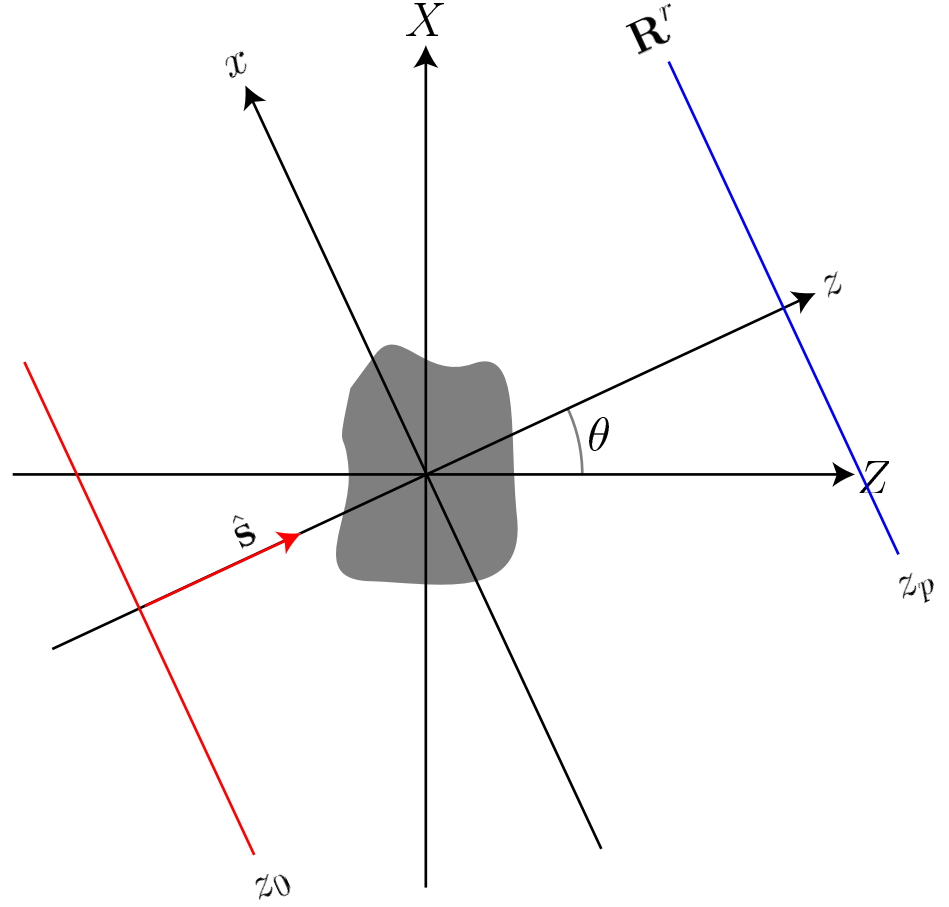\tag{54}
$$

3.1 Plane Wave Details & Fourier Diffraction Theorem

The forward scattering model is given by the approximation of Eqn. 50:

$$
U^{scat}(\mathbf{R}^r, \hat{\mathbf{s}}) = C(\mathbf{R}^r) \, P(\omega) \, k_0^2 \int d\mathbf{r}' \, G_0(\mathbf{R}^r, \mathbf{r}', \omega) \, o(\mathbf{r}') \, e^{ik_0 \hat{\mathbf{s}} \cdot \mathbf{r}'},
\tag{55}
$$

where we now explicitly state the background Green function

$$
G_0(\mathbf{R}^r, \mathbf{r}', \omega) = \frac{e^{ik_0 |\mathbf{R}^r - \mathbf{r}'|}}{4\pi |\mathbf{R}^r - \mathbf{r}'|},
\tag{56}
$$

Figure 1: *Schematic of measurement system. The plane wave propagation vector,* $\hat{\mathbf{s}}$, *is given by* $(\sin\theta, 0, \cos\theta)$ *in the fixed object coordinate system. The point source location is given by* $z_0\,(\sin\theta, 0, \cos\theta)$ *in the fixed coordinate system. The entire measurement system rotates about the* y*-axis which is out of the plane of the page.*

and

$$k_0 \equiv \frac{\omega}{c_0} \tag{57}$$

is the background wave number. Substitute the Weyl expansion,

$$\frac{e^{ik_0|\mathbf{R}^r - \mathbf{r}'|}}{4\pi\,|\mathbf{R}^r - \mathbf{r}'|} = \frac{i}{8\pi^2} \int d\mathbf{k}'_\perp \frac{e^{i\left(\mathbf{k}'_\perp \cdot (\mathbf{r}_\perp - \mathbf{r}'_\perp) + \gamma(\omega)|z_p - z'|\right)}}{\gamma(\omega)}, \tag{58}$$

where $\gamma(\omega) \equiv \sqrt{k_0^2 - |\mathbf{k}'_\perp|^2}$, and $\mathbf{R}^r \equiv (\mathbf{r}_\perp, z_p)$, into Eqn. 55

$$U^{scat}(\mathbf{R}^r, \hat{\mathbf{s}}) = \frac{i\,C(\mathbf{R}^r)\,P(\omega)\,k_0^2}{8\pi^2} \int d\mathbf{r}' \int d\mathbf{k}'_\perp \frac{e^{i\mathbf{k}'_\perp \cdot (\mathbf{r}_\perp - \mathbf{r}'_\perp) + \gamma(\omega)|z_p - z'|}}{\gamma(\omega)}\, o(\mathbf{r}')\, e^{ik_0(\omega)\hat{\mathbf{s}}\cdot\mathbf{r}'}. \tag{59}$$

We note that for the transmission mode measurement system depicted in Figure 1, $z_p > z'$ so that we may set

$$|z_p - z'| = z_p - z' \tag{60}$$

to achieve

$$
\begin{aligned}
U^{scat}(\mathbf{R}^r, \hat{\mathbf{s}}) &= \frac{i\,C(\mathbf{R}^r)\,P(\omega)\,k_0^2}{8\pi^2} \int d\mathbf{r}' \int d\mathbf{k}'_\perp \frac{e^{i\left(\mathbf{k}'_\perp \cdot (\mathbf{r}_\perp - \mathbf{r}'_\perp) + \gamma(\omega)(z_p - z')\right)}}{\gamma(\omega)}\, o(\mathbf{r}')\, e^{ik_0(\omega)z'}, \\
&= \frac{i\,C(\mathbf{R}^r)\,P(\omega)\,k_0^2}{8\pi^2} \int \frac{d\mathbf{k}'_\perp}{\gamma(\omega)}\, e^{i\left(\mathbf{k}'_\perp \cdot \mathbf{r}_\perp + \gamma(\omega)z_p\right)} \times \\
&\quad \int d\mathbf{r}'\, o(\mathbf{r}')\, e^{-i\left(\mathbf{k}'_\perp \cdot \mathbf{r}'_\perp - (k_0(\omega) - \gamma(\omega))z'\right)}.
\end{aligned} \tag{61}
$$

Using the spatial Fourier transform pair definitions from Appendix A,

$$\tilde{\psi}(\mathbf{k}) = \int d\mathbf{r}\, \psi(\mathbf{r})\, e^{-i\mathbf{k}\cdot\mathbf{r}}, \tag{62}$$

$$\psi(\mathbf{r}) = \frac{1}{(2\pi)^n} \int d\mathbf{k}\, \tilde{\psi}(\mathbf{k})\, e^{i\mathbf{k}\cdot\mathbf{r}}, \tag{63}$$

where n is the dimensionality of the transform, we conclude the $\mathbf{r}'$ integral in Eqn. 61 is the spatial Fourier transform of the object:

$$O\left(\mathbf{k}'_\perp, k'_z\right) = \int d\mathbf{r}'\, o(\mathbf{r}')\, e^{-i\left(\mathbf{k}'_\perp \cdot \mathbf{r}'_\perp - (k_0 - \gamma(\omega))z'\right)}, \tag{64}$$

where $k'_z \equiv -(k_0 - \gamma(\omega))$. Eqn. 61 then reads

$$U^{scat}(\mathbf{r}_\perp, z_p, \hat{\mathbf{s}}) = \frac{i\,C(\mathbf{R}^r)\,P(\omega)\,k_0^2}{8\pi^2} \int \frac{d\mathbf{k}'_\perp}{\gamma(\omega)}\, e^{i\left(\mathbf{k}'_\perp \cdot \mathbf{r}_\perp + \gamma(\omega)z_p\right)}\, O\left(\mathbf{k}'_\perp, k'_z\right). \tag{65}$$

9

We digress briefly to examine the $C(\mathbf{R}^r)$ factor under the Born and Rytov approximations. We have

$$
C(\mathbf{R}^r) = \begin{cases} 1 & \text{for the Born approximation,} \\[2ex] \dfrac{1}{\psi^{inc}(\mathbf{r})} = \dfrac{e^{-ik_0\hat{\mathbf{s}}\cdot\mathbf{R}^r}}{P(\omega)} = \dfrac{e^{-ik_0 z_p}}{P(\omega)} & \text{for the Rytov approximation.} \end{cases}
\tag{66}
$$

We note $C(\mathbf{R}^r)$ is independent of the planar measurement variable $\mathbf{r}_\perp$. This is significant because we now perform a planar Fourier transform (PFT) of the measured scattered quantity[1],

$$
\begin{aligned}
\bar{U}^{scat}(\mathbf{k}_\perp, z_p, \hat{\mathbf{s}}) &= \int d\mathbf{r}_\perp \, U^{scat}(\mathbf{r}_\perp, z_p, \hat{\mathbf{s}}) \, e^{-i\mathbf{k}_\perp \cdot \mathbf{r}_\perp}, \\
&= \frac{i\, C(\mathbf{R}^r)\, P(\omega)\, k_0^2}{8\pi^2} \times \\
& \quad \int \frac{d\mathbf{k}'_\perp}{\gamma(\omega)} \left[\int d\mathbf{r}_\perp \, e^{i\left(\mathbf{k}'_\perp - \mathbf{k}_\perp\right)\cdot\mathbf{r}_\perp} \right] e^{i\gamma(\omega)z_p} \, O\left(\mathbf{k}'_\perp, k'_z\right).
\end{aligned}
\tag{67}
$$

We use the identity

$$
\delta\left(\mathbf{k}'_\perp - \mathbf{k}_\perp\right) = \frac{1}{(2\pi)^{n-1}} \int d\mathbf{r}_\perp \, e^{i\left(\mathbf{k}'_\perp - \mathbf{k}_\perp\right)\cdot\mathbf{r}_\perp},
\tag{68}
$$

to reduce Eqn. 67 to

$$
\bar{U}^{scat}(\mathbf{k}_\perp, z_p, \hat{\mathbf{s}}) = \frac{i\, C(\mathbf{R}^r)\, P(\omega)\, k_0^2 \, e^{i\gamma(\omega)z_p}}{2\gamma(\omega)} \, O\left(\mathbf{k}_\perp, k_z\right).
\tag{69}
$$

Eqn. 69 relates the n-dimensional Fourier transform of the object to the $(n-1)$-dimensional planar transform of the measured scattered field (Born approximation) or the measured scattered phase (Rytov approximation). It is known as the *Fourier Diffraction Theorem* in wave-based tomography and is the equivalent of the *Fourier Slice Theorem* [10] of straight-ray tomography. Explicitly, we have the measured field (phase) on the $\mathbf{k}_\perp$ plane which is proportional to the object Fourier transform in the $(\mathbf{k}_\perp, k_z)$ space. This appears at first to be a mapping from an n-dimensional function to a $(n-1)$-dimensional function. Note, however, that k_z depends upon $\mathbf{k}_\perp$ via

$$
k_z \equiv -\left(k_0 - \sqrt{k_0^2 - |\mathbf{k}_\perp|^2}\right).
\tag{70}
$$

Thus, the relationship is a mapping of the $(n-1)$-dimensional locus of points through the n-dimensional space described by $(\mathbf{k}_\perp, k_z)$, to the $(n-1)$-dimensional Fourier space measurement plane. Applying the coordinate rotation of Eqn. 54 to account for all measurement angles θ, we

---

[1] Amplitude in the Born approximation or phase in the Rytov approximation

have in the fixed object frame

$$
\begin{bmatrix} K_x \\ K_y \\ K_z \end{bmatrix} = \begin{bmatrix} \cos\theta & 0 & \sin\theta \\ 0 & 1 & 0 \\ -\sin\theta & 0 & \cos\theta \end{bmatrix} \begin{bmatrix} k_x \\ k_y \\ -(k_0 - \gamma(\omega)) \end{bmatrix},
$$

$$
= \begin{bmatrix} k_x\cos\theta + (k_0 - \gamma(\omega))\sin\theta \\ k_y \\ -k_x\sin\theta - (k_0 - \gamma(\omega))\cos\theta \end{bmatrix}, \tag{71}
$$

where we have explicitly used the dependence of k_z on k_0 and $\mathbf{k}_\perp \equiv (k_x, k_y)$. Curves of $K_x(k_x)$ and $K_z(k_x)$ are presented in Figure 2 for multiple values of θ with $|k_x| \le k_0$. This constraint on k_x, or more generally the constraint that $|\mathbf{k}_\perp| \le k_0$ is required to ensure k_z remain real valued as can be observed in Eqn. 70. For $|\mathbf{k}_\perp| > k_0$, k_z becomes complex and the resulting fields evanescent. Although evanescent field tomography is possible, given the dimensions of the measurement system with respect to the illuminating wavelength, it is not practical because no evanescent field will reach the measurement plane.

Although our entire development has been in n-dimensions (for all intents, three dimensions), the Fourier Diffraction Theorem is entirely two dimensional. Eqn. 71 shows the relationship between the K_y and k_y dimensions to be one-to-one. That is, the mapping is one-to-one in the Fourier variable complementary to the axis of rotation. Thus, in the three Fourier dimensions, the loci of points plotted in Figure 2 form a cylinder along the k_y axis, perpendicular to the plane of the page.

The Fourier Diffraction Theorem dictates the resolution of the reconstruction. Assume evanescent fields are neglected, the resolution limit is governed by the Ewald sphere [8, 9] which indicates the transition from propagating to evanescent fields. For this case of narrow-band transmission mode tomography, this limit is inversely proportional to $\sqrt{2}k_0$. Consider the spatial frequency limit in inverse length (as opposed to radians),

$$
\begin{aligned}
\sqrt{2}\eta &\equiv \sqrt{2}\sqrt{\eta_x^2 + \eta_z^2}, \\
&= \sqrt{2}\frac{k_0}{2\pi}, \\
&= \sqrt{2}\frac{f}{c_0}, \\
&= \frac{\sqrt{2}}{\lambda},
\end{aligned} \tag{72}
$$

where we have used Eqn. 57, $\omega = 2\pi f$, and $c_0 = f\lambda$, where f is the frequency of the illuminating source. The spatial resolution limit is thus $\lambda/\sqrt{2}$ in the plane of rotation. In the perpendicular domain, the resolution limit is governed by the spatial sampling along the y-axis.

We are now prepared to invert Eqn. 69 in order to "reconstruct" the scattering object. In theory it is a simple matter of solving for the object spectrum and performing an inverse Fourier transform. However, we do not know the object's spectrum on a Cartesian grid: we know it at the points defined by Eqn. 71. Furthermore, lower spatial frequencies are sampled more densely by the Fourier Diffraction Theorem than higher ones, with the zero frequency (that is, DC) being sampled
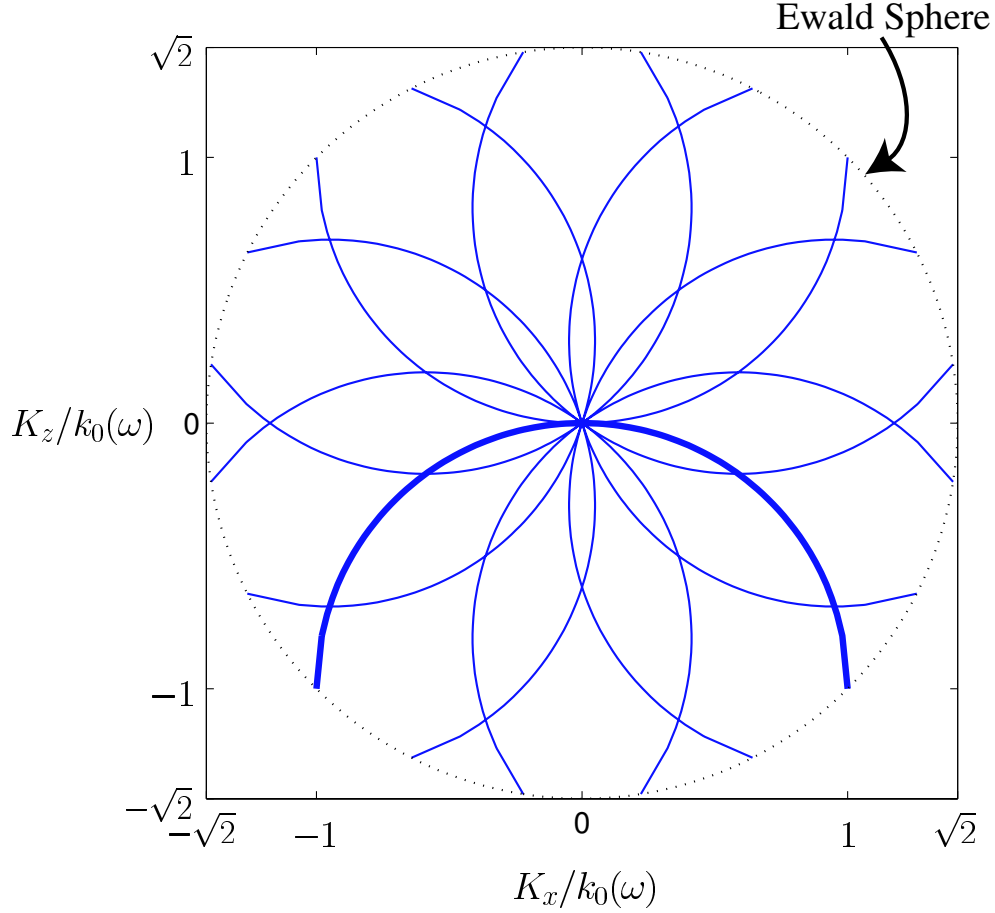
11

Figure 2: *Graphical representation of the Fourier Diffraction Theorem of Eqn. 69. The curves represent the loci of points given by Eqn. 71 in the object's Fourier space. The Ewald sphere defines the transition from propagating to evanescent field spectra.*

the most: all curves pass through the origin. We account for these issues and develop an inverse in the next section.

3.2 Plane Wave Inversion

Solving for the object spectrum of Eqn. 69 yields

$$O\left(\mathbf{k}_{\perp}, k_z\right) = -\frac{i\,2\gamma(\omega)\,e^{-i\gamma(\omega)z_p}}{C(\mathbf{R}^r)\,P(\omega)\,k_0^2}\,\bar{U}^{scat}(\mathbf{k}_{\perp}, z_p, \hat{\mathbf{s}}), \qquad (73)$$

in terms of the PFT of the measured scattered field.

For practical considerations, we neglect the evanescent field information and limit ourselves to the propagating spectrum of $|\mathbf{k}_{\perp}| \leq k_0$. This yields a low pass reconstruction of the object as

12

indicated by the spectral coverage of Figure 2. We define the unit step function by

$$S(k) \equiv \begin{cases} 0 & k < 0 \\ 1 & k \geq 0, \end{cases} \tag{74}$$

and write

$$O_{lp}(\mathbf{k}_\perp, k_z) = -\frac{i \, 2\gamma(\omega) \, e^{-i\gamma(\omega)z_p}}{C(\mathbf{R}^r) \, P(\omega) \, k_0^2} \, \bar{U}^{scat}(\mathbf{k}_\perp, z_p, \hat{\mathbf{s}}) \, S\left(k_0 - |\mathbf{k}_\perp|\right), \tag{75}$$

where the *lp* subscript indicates we will be performing a low pass reconstruction.

We are now prepared to define the inverse Fourier transform of Eqn. 75 to obtain the low pass object reconstruction. The inverse Fourier transform is

$$\hat{o}(\mathbf{R}) = \frac{1}{(2\pi)^n} \int d\mathbf{K} \, O_{lp}(\mathbf{K}) \, e^{i\mathbf{K}\cdot\mathbf{R}}, \tag{76}$$

where $\mathbf{K}$ is given by Eqn. 71. The object spectrum of Eqn. 76 is specified in terms of the Cartesian coordinate system given by $\mathbf{K} = (K_x, K_y, K_z)$. The actual measured values of the spectrum are known along the arcs given by

$$\begin{bmatrix} K_x \\ K_y \\ K_z \end{bmatrix} = \begin{bmatrix} k_x \cos\theta + (k_0 - \gamma(\omega))\sin\theta \\ k_y \\ -k_x \sin\theta - (k_0 - \gamma(\omega))\cos\theta \end{bmatrix}. \tag{77}$$

In order to perform the integral of Eqn. 76, we must change the integration variables from the object spectrum's Cartesian frame to those of the rotated frame of the incident plane wave. The Jacobian of the transformation is

$$J(\mathbf{K};\mathbf{k}) = \begin{vmatrix} \partial K_x/\partial k_x & \partial K_y/\partial k_x & \partial K_z/\partial k_x \\ \partial K_x/\partial k_y & \partial K_y/\partial k_y & \partial K_z/\partial k_y \\ \partial K_x/\partial k_z & \partial K_y/\partial k_z & \partial K_z/\partial k_z \end{vmatrix} = \frac{k_0 \, k_x}{\gamma(\omega)}. \tag{78}$$

We now express the inverse Fourier transform as

$$\hat{o}(\mathbf{R}) = \frac{-i2}{(2\pi)^n \, C(\mathbf{R}^r) \, P(\omega) \, k_0} \int\limits_{|\mathbf{k}_\perp| < k_0} d\mathbf{k}_\perp \, |k_x| \, e^{-i\gamma(\omega)z_p} \int_0^{2\pi} d\theta \, \bar{U}^{scat}(\mathbf{k}_\perp, z_p, \hat{\mathbf{s}}) \, e^{i\mathbf{k}\cdot\mathbf{r}}, \tag{79}$$

where we have used Eqns. 54 and 73.

$$\hat{o}(\mathbf{R}) = \frac{-i2 \, e^{-ik_0 z_p}}{(2\pi)^n \, C(\mathbf{R}^r) \, P(\omega) \, k_0} \int_0^{2\pi} d\theta \int_{-\infty}^{\infty} d\mathbf{k}_\perp \, H(\mathbf{k}_\perp, z - z_p) \, \bar{U}^{scat}(\mathbf{k}_\perp, z_p, \hat{\mathbf{s}}) \, e^{i\mathbf{k}_\perp \cdot \mathbf{r}_\perp}, \tag{80}$$

where

$$H(\mathbf{k}_\perp, z) \equiv |k_x| \, e^{-i(k_0 - \gamma(\omega))z} \, S\left(k_0 - |\mathbf{k}_\perp|\right). \tag{81}$$

13

Eqn. 80 is the "standard" filtered backpropagation algorithm [9]. The $|k_x|$ expression represents a filter which accounts for the non-uniform sampling of the Fourier Diffraction Theorem. The product $e^{-ik_0 z_p} e^{-i(k_0 - \gamma(\omega))z}$ represents a plane-to-plane backpropagation of the measured quantity from the measurement plane to a plane within the object. Finally, the $S(k_0 - |\mathbf{k}_\perp|)$ expression imposes the low-pass limit of the reconstruction require to remove evanescent fields which, when backpropagated, diverge given their exponentially decaying nature in the forward propagation direction.

4 Summary & Conclusions

We have developed a wave-based inversion and imaging algorithm which is applicable to the Optical Quadrature Microscope. We have assumed narrow-band plane wave illumination of the object under evaluation. We have also assumed multiple planar measurements, uniformly distributed $360°$ about the object, are possible while maintaining a fixed object to measurement plane distance.

References

[1] D. O. Hogenboom and C. A. DiMarzio. Quadrature detection of a doppler signal. *Applied Optics*, **13**(13):2569–2572, May 1998.

[2] D. O. Hogenboom, C. A. DiMarzio, T. J. Gaudette, A. J. Devaney, and S. C. Lindberg. Three-dimensional images generated by quadrature interferometry. *Optical Society of America*, **23**(10):783–785, May 1998.

[3] Y. Glina, G. A. Tsihrintzis, C. M. Warner, D. O. Hogenboom, and C. A. DiMarzio. On the use of the optical quadrature method in tomographic microscopy. In *SPIE Conference on Three-Dimensional and Multidimensional Microscopy: Image Acquisition and Processing VI*, volume **3605**, pages 101–106. SPIE, January 1999.

[4] D. J. Townsend, K. D. Quarles, A. L. Thomas, W. S. Rockward, C. M. Warner, J. A. Newmark, and C. A. DiMarzio. Quantitative phase measurements using a quadrature tomographic microscope. In T. Wilson J.-A. Conchello, C. J. Cogswell, editor, *Three-Dimensional and Multidimensional Microscopy: Image Acquisition and Processing X*, volume **4964**, pages 59–65. SPIE, 2003.

[5] II W. C. Warger. The fusion of optical quadrature and differential interference contrast microscopy to produce accurate cell counts in live mouse embryos. Master's thesis, Northeastern University, 2005.

[6] J. D. Jackson. *Classical Electrodynamics*. John Wiley & Sons, Inc., 3nd edition, 1999. ISBN 0-471-30932-X.

[7] G. Beylkin and M. L. Oristaglio. Distorted-wave born and distorted-wave rytov approximations. *Optics Communications*, **53**(4):213–216, March 1985.

[8] M. Born and E. Wolf. *Principles of Optics*. Cambridge University Press, 7th edition, 1999. ISBN 0-521-642221.

[9] A. J. Devaney. A filtered backpropagation algorithm for diffraction tomography. *Ultrasonic Imaging*, **4**(4):336–350, October 1982.

[10] A. C. Kak and M. Slaney. *Principles of Computerized Tomographic Imaging*. IEEE Press, 1988. ISBN 0-7803-0447-0.

A Standard Fourier Transforms

We summarize without comment our Fourier transform definitions.

Forward in time

$$U(\mathbf{r}, \omega) \;=\; \int_{-\infty}^{\infty} dt\, u(\mathbf{r}, t)\, e^{i\omega t}$$

Inverse in time

$$u(\mathbf{r}, t) \;=\; \frac{1}{2\pi} \int_{-\infty}^{\infty} d\omega\, U(\mathbf{r}, \omega)\, e^{-i\omega t}$$

Forward in space

$$\tilde{U}(\mathbf{k}, \omega) \;=\; \int_{-\infty}^{\infty} d\mathbf{r}\, U(\mathbf{r}, \omega)\, e^{-i\mathbf{k}\cdot\mathbf{r}}$$

Inverse in space

$$U(\mathbf{r}, \omega) \;=\; \frac{1}{(2\pi)^3} \int_{-\infty}^{\infty} d\mathbf{k}\, \tilde{U}(\mathbf{k}, \omega)\, e^{i\mathbf{k}\cdot\mathbf{r}}$$